

This is the accepted manuscript made available via CHORUS. The article has been published as:

Spontaneous propagation of self-assembly in a continuous medium

Zhouzhou Zhao and Wei Lu

Phys. Rev. E **85**, 041124 — Published 17 April 2012

DOI: [10.1103/PhysRevE.85.041124](https://doi.org/10.1103/PhysRevE.85.041124)

Spontaneous Propagation of Self-Assembly in a Continuum Medium

Zhouzhou Zhao and Wei Lu*

Department of Mechanical Engineering, University of Michigan, Ann Arbor, Michigan

48109

ABSTRACT

We report a mechanism that self-assembly propagates spontaneously in a continuum medium, enabling the delivery of local order information to distance. In a large stable system a locally self-assembled structure as a precursor destabilizes its surrounding areas through a dipole interaction. The newly formed structures inherit the same order information from the precursor and further activate the self-assembly of their neighbors. This process causes spatial extension of self-assembly and replication of the order, producing extremely long-range ordered superlattice without defects.

* To whom correspondence should be addressed: weilu@umich.edu

I. INTRODUCTION

Self-assembly, the spontaneous organization of components into ordered patterns or structures[1], is ubiquitous in nature. Inspired by its elegance, researchers are exploring the concept to form useful structures for advanced materials[2], electronic nano-devices[3] and solar cells[4]. Depending on the building blocks, self-assembly systems can be categorized into two types: discrete and continuum. A discrete system utilizes pre-fabricated building blocks such as nanoparticles[5, 6] and nanorods[7, 8]. These components, with fixed sizes and shapes, aggregate into ordered crystal-like structures. In contrast, a continuum system exploits the spontaneous formation of nanoscale domains. The domain size and shape are not pre-fabricated, but emerge during the self-assembly process. A continuum system offers several advantages. For instance, domains and their patterns self-assemble simultaneously, so that there is no need to pre-synthesize the building blocks. A significant degree of process flexibility and control can be achieved. The approach may be applied to diverse systems, such as microphase separation of block-copolymers[9, 10], spinodal decomposition of binary monolayers [11, 12] and ordered pattern of organic molecules[13, 14].

While self-assembly holds great potential for nanofabrication, people have yet to find a general and intrinsic approach to effectively control the appearance of defects in the formed structures. Homogeneous phase separation in a continuum self-assembling system is the origin of defects, which are prone to appear when multiple grains emerging at different locations meet. Top-down approach has been investigated to help reduce defect formation by regulating the orientations of grains through physical masks[15, 16] or templates of external fields [10, 17, 18].

In this paper, we show that extremely long-range ordered nanostructures can form without any external assistance by spontaneous propagation of self-assembly.

Propagation phenomena are widely observed in nature and human activities. Examples include solidification[19], tumor growth[20], frontal polymerization of actin[21], chemical chain reaction[22], to population dynamics[23]. These phenomena can usually be described by the general diffusion-reaction model[24] with corresponding reaction terms. Moreover, these processes usually begin with a stage small in extent and then propagate over a large area. In contrast, self-assembled patterns are usually formed large in extent with no propagation.

The question we aim to address is: can self-assembly propagate? Is it possible for a system to self-assemble locally to form a regular domain pattern, and then replicate this pattern spontaneously to distance? We envision a mechanism as below. Consider a homogeneous system stable against small perturbation so that self-assembly does not occur spontaneously. Upon activation of self-assembly in a local region, the formed ordered pattern may produce sufficient destabilizing effect through long-range interaction to trigger self-assembly in its immediate surrounding areas. The newly formed structures inherit the same order information and further destabilize their neighbors. The chain reaction may propel the propagation of self-assembly into distance and generate an extreme long-range order.

There are few studies on the propagation of self-assembly on its strict definition. Some research has considered self-assembly in the loose sense, which refers to the aggregation of building blocks without forming any ordered pattern. For example, propagating aggregation waves were demonstrated in an organosilane monolayer system[25]. The organic molecules aggregated when the concentration was higher than a critical value. The propagation was driven

by concentration gradient. In another experimental study, the propagation of patterns in Langmuir monolayer at liquid-air interface was shown[26]. A local disturbance was driven by a constant external light excitation and the propagation was maintained via elastic forces. Although propagation phenomenon was reported in these systems, there were no explicit ordered patterns formed. We show that the propagation of self-assembly can carry ordering information and transmit it through intrinsic interaction between domains.

II. MODEL

Many continuum self-assembly systems demonstrate similar domain patterns, which suggests a possible universal theoretical framework. Here we consider a representative system with dipole-type interaction, which can be physically originated from electrostatic[27], magnetic[28] or elastic[29, 30] interactions. Experiments have shown periodic dots or other domain patterns in these self-assembly systems, with domain size in the range of 1-100nm[11].

Consider a thin film of two atomic species A and B. Define $C(\mathbf{x})$ as the position dependent concentration fraction, $C=0$ for pure A and $C=1$ for pure B. A homogeneous film may phase separate to form A-rich and B-rich domains. The free energy involves short-range atomic interaction and long-range interaction between domains, namely $G = \int_A f(C)dA + h \int_A |\nabla C|^2 dA - \mu^2 / 2 \int_A \int_{A'} C(\mathbf{x})g(\mathbf{x}, \mathbf{x}')C(\mathbf{x}')dAdA'$. The first term is relevant to phase separation, where $f(C)$ is the chemical energy per unit area, which represents the excess energy of mixing. The second term is the phase boundary energy, which prefers a larger domain size. The material parameter h is a positive constant. The third term captures the

long-range nature of dipole-dipole interaction, where $g(\mathbf{x}, \mathbf{x}') = |\mathbf{x} - \mathbf{x}'|^{-3}$ and μ is the dipole density difference between pure A and B domains. The negative sign comes from Legendre transformation for a fixed average concentration. This term prefers a smaller domain size. The two actions compete and determine the domain size. The reduction of the free energy drives diffusion and leads to pattern formation. Take elastic dipole interaction induced by surface stress as an example, the normalized diffusion equation is [29]

$$\frac{\partial C}{\partial t} = \nabla^2 \left[\frac{df}{dC} - 2\nabla^2 C + QI \right]. \quad (1)$$

Here Q is a dimensionless number scales with the ratio of interface width and domain size. I is an area integration over the substrate surface characterizing the long-range interaction, namely

$$I = -\frac{1}{\pi} \iint \frac{(x-\xi) \frac{\partial C}{\partial \xi} + (y-\eta) \frac{\partial C}{\partial \eta}}{\left[(x-\xi)^2 + (y-\eta)^2 \right]^{3/2}} d\xi d\eta, \quad (2)$$

where ξ and η are coordinates and variables of integration.

The condition of self-assembly can be obtained from linear stability analysis. Assume a regular solution $f(C) = C \ln C + (1-C) \ln(1-C) + \Omega C(1-C)$, where Ω is a dimensionless number measuring the bond strength relative to the thermal energy. The curve $f(C)$ is convex and prefers a homogenous film when $\Omega < 2$. Consider a perturbation of the form $C(x, t) = C_0 + q(t) \sin(kx)$, where C_0 is the average concentration. The solution of Eq. (1) is $q = q_0 e^{\alpha t}$, where q_0 is the initial amplitude and $\alpha = k^2 [-1 / [C_0(1-C_0)] + 2\Omega - 2k^2 + 2Qk]$. With $\alpha \leq 0$ for all k , the perturbation amplitude q decays with time so that a homogeneous film is

stable against small perturbation. This condition corresponds to $C_0 \leq C_L$ or a symmetric case of $C_0 \geq C_H$, where $C_L = (1 - \sqrt{1-s})/2$, $C_H = (1 + \sqrt{1-s})/2$, and $s = 8/(Q^2 + 4\Omega)$. Self-assembly occurs for $C_L < C_0 < C_H$. With $\Omega=1.3$ and $Q=1.8$ we have $C_L = 0.386$ and $C_H = 0.614$.

III. RESULTS AND DISCUSSION

Unlike common study of self-assembly in the regime of $C_L < C_0 < C_H$, here we focus on the stable regime of $C_0 \leq C_L$. Figure 1 demonstrates how self-assembly can propagate under such a condition. We performed fully non-linear simulation of Eq. (1) in Fourier space with periodic boundary directions. The initial condition was set to fluctuate randomly within 0.001 from an average. We took $\Omega=1.3$ and $Q=1.8$. The film was initially homogeneous with an average concentration of $C_0=0.38$ (below C_L), which was stable against small perturbation. We introduced a small initiation zone at the left edge by increasing its local concentration to 0.42 (above C_L) for self-assembly to occur. The width of the rectangular initiation zone is roughly the diameter of a self-assembled dot. This ensures that an array of dots is aligned along the y axis. In experiments we envision that this process can be achieved by local mass deposition. The size of the initiation zone may be as large as a single grain so that no defects are introduced. A typical grain contains about 10 dots across its diameter. Upon pattern formation, the nearby homogeneous region was disturbed and became unstable. Self-assembly propagated and generated a uniform lattice of dots in the entire film without any defects. To eliminate the boundary effect, the presented results were cropped from a larger calculation cell of 2048×48 . We placed the initiation zone in the middle of the stripe so that self-assembly actually

propagated symmetrically toward two sides. The right 512×48 was shown in Fig. 1. The intriguing propagation poses interesting questions. Why does self-assembly propagate and what determines the rate? How can we control the propagation process?

While we started self-assembly in a small initiation zone by giving it a concentration higher than C_L , this amount had negligible effect on the average concentration of the entire film. Thus the propagation was not due to the long-range diffusion of higher concentration. We believe that the self-sustained propagation relies on the interaction between the ordered structure in the propagation front and the homogenous region immediately ahead of it, which we call affected zone. Equation (2) shows that the I term is negligible when the film is homogeneous with small random noise. In contrast, the self-assembled pattern in the propagation front induces a dipole-type I field that is in phase with the pattern and extends into the affected zone, as shown in Fig. 1. How this field triggers self-assembly propagation is related to the free energy.

For a hexagonal pattern of dots lining up along the y direction with a lattice space of d , as shown in the inset of Fig. 2a, the concentration field can be represented by

$$C(x, y) = C_0 + \sum_m q_{m0} \cos\left(m \frac{2\pi x}{\sqrt{3}d}\right) + \sum_n q_{0n} \cos\left(n \frac{2\pi y}{d}\right) + \sum_{m,n} q_{mn} \cos\left(m \frac{2\pi x}{\sqrt{3}d}\right) \cos\left(n \frac{2\pi y}{d}\right) \quad (3)$$

The summations run from 1 to ∞ . Minimization of the free energy in terms of d gives the equilibrium size, $d = 4\pi S / QH$ and free energy per area, $g = L - Q^2 H^2 / 8S$. Here

$$S = \sum_m m^2 q_{m0}^2 / 3 + \sum_n n^2 q_{0n}^2 + 1/2 \sum_{m,n} (m^2 / 3 + n^2) q_{mn}^2 \quad \text{and}$$

$$H = \sum_m m q_{m0}^2 / \sqrt{3} + \sum_n n q_{0n}^2 + 1/2 \sum_{m,n} q_{mn}^2 \sqrt{m^2 / 3 + n^2} \quad \text{depend only on the geometry, and not}$$

the scale, of the patterns, while $L = \int_{-1/2}^{1/2} \int_{-1/2}^{1/2} [C \ln C + (1-C) \ln(1-C) + \Omega C(1-C)] d\xi d\eta$, $\xi = x/\sqrt{3}d$, $\eta = y/d$. We further minimize g with respect to q_{m0} , q_{0n} , and q_{mn} by the conjugate-gradient method to obtain the free energy per area of a hexagonal lattice of dots, as shown in Fig. 2a. For a homogenous film the free energy density is simply L evaluated at C_0 . The hexagonal pattern has lower energy than a homogenous film when the concentration is higher than a critical value, C_D . The range between C_D and C_L creates a special bistable state, where a homogenous film is stable against small perturbation yet the hexagonal pattern has lower energy. The concentration C_0 in Fig. 1 falls in this bistable state. As illustrated in Fig. 2b, self-assembly from a homogenous film (H) to the dot pattern (D) will reduce the free energy by Δg_{H-D} , but it needs help to first overcome an energy barrier, Δg_b .

The ordered pattern in the growth front helps to eliminate the energy barrier in the affected zone by the I field, which modulates in y and decays quickly in x . We approximate the field by $I_a(x, y) = \sum_l a_l \cos(2\pi l y/d + \theta) e^{-kx}$, where a_l is amplitude, θ is the phase angle relative to the perturbation to be examined in the affected zone and k is a decay parameter. Due to its proximity to an ordered pattern, a homogenous film perturbed in the affected zone by the form of Eq. (3) has an additional free energy per area,

$$\Delta g_a = -\frac{(1 - e^{-\sqrt{3}kd})Q}{2\sqrt{3}kd} \sum_n a_n \cos \theta \left[q_{0n} + \sum_m \frac{q_{mn}}{1 + (2m\pi / \sqrt{3}kd)^2} \right]. \quad (4)$$

The negative Δg_a promotes the destabilization of a homogenous film by more energy reduction. In addition, Δg_a minimizes at $\theta = 0$, suggesting that any emerging pattern will prefer to be in

phase with I_a or the existing pattern in the growth front. This effect explains why the subsequent dot pattern follows the same orientation and extremely long-range ordered lattice can form. The term Δg_a is also proportional to the perturbation amplitudes q_{0n} and q_{mn} , suggesting more energy reduction as the pattern grows. Self-assembly in the affected zone occurs when Δg_a removes the energy barrier. Then the following propagation appears like an autocatalytic process transitioning from a homogenous film to a dot pattern, or $H \xrightarrow{D} D$.

The propagation process may be accompanied by a significant gradient-driven long-range diffusion if the average concentration of the dot pattern, C_p , is quite different from C_0 . This situation may happen since a dot pattern can reach lower free energy if it raises its average concentration above C_0 , as shown by the monotonic curve in Fig. 2a. To maintain an overall C_0 , the homogenous film ahead of the growth front has to reduce its average concentration, which increase its free energy. After a balance is reached, a region with an average concentration C_a ($C_a < C_0$) is formed ahead of the growth front, as illustrated in the inset of Fig. 3. Then the concentration gradient drives long-range diffusion from the remote area in the homogenous film to the affected zone by a diffusion distance d . The lower C_a in the affected zone makes it more stable since it is further from C_L .

The long-range diffusion is necessary to sustain the pattern growth when it maintains an average concentration higher than C_0 . The accumulated concentration relocation to the dot pattern increases as it expands. Thus the diffusion distance or the front width, d , increases with the propagation of self-assembly. The diffusion rate reduces as a result of the decreasing

concentration gradient, $(C_0 - C_a)/d$, which slows down the propagation of self-assembly. This trend can be clearly observed through the decreasing slope of the $Q=1.7$ curve in Fig. 3. We have found an effective approach to control the propagation rate by tuning how much it is limited by long-range diffusion. The triggering I field from the growth front affects how fast self-assembly emerges in the affected zone, while the long-range diffusion affects how fast the mass transport is. Thus the propagation would be faster for a larger triggering field and minimal requirement of long-range diffusion, which translate to larger Q and smaller Ω . The $f(C)$ curve is more steep for smaller Ω , thus makes it more energetically unfavorable for a uniform film to decrease its concentration for a higher average concentration of the dot pattern. Therefore the dot pattern would maintain an average concentration close to C_0 and does not need much long-range diffusion during propagation. As shown in Fig. 3, the propagation slows down significantly with $Q=1.7$, $\Omega=1.4$, while keeps an almost constant rate with $Q=1.8$, $\Omega=1.3$. Generally speaking, we can classify the propagation of self-assembly into two modes: long range diffusion-limited and activation-limited. The former situation is similar to many frontal propagations [21, 25, 31], when the fronts move forward at the cost of background concentration. For actin polymerization, the propagation stops automatically when the surrounding concentration decreases to a critical value. To prevent the cease of propagation, one could manually keep the background concentration invariant by constantly adding reactive materials [25]. The latter involves little or no long-range diffusion, and is determined only by the local transport for concentration modulation. Without the requirement of the mass replenishment, this scenario is unique and preferred for potential large-scale nanofabrication. Propagation can also happen in two-

dimensions, as demonstrated in Fig. 4. Starting with a circular initiation zone, the hexagonal pattern quickly expands to the entire area. Defect-free patterns are produced in a high output manner.

In real systems, temperature and fluctuation can affect the propagation. With increasing temperature, a higher propagation rate is generally expected due to higher mobility. Thermal fluctuation usually causes the broadening of the front width in a typical propagating system[32]. To consider the fluctuation effect, a random “white noise” term $\varepsilon(\mathbf{x}, t)$ can be added to the right hand side of Eq. (1). This random term obeys the fluctuation dissipation theorem so that $\langle \varepsilon(\mathbf{x}, t) \varepsilon(\mathbf{x}', t') \rangle$ scales with $k_b T \delta(\mathbf{x} - \mathbf{x}') \delta(t - t')$, where k_b is Boltzmann’s constant, and T is the absolute temperature [33]. The fluctuation is small compared to the average concentration, and therefore has minimum effect on the equilibrium size of the domains, as can be seen from the derived dispersion relation $\alpha(k)$. In our system the dipole interaction dominates at the propagation front, thus the fluctuation would not significantly affect the growth front width.

It should be noted that similar propagation phenomena were reported in reaction-diffusion experiments [34]. The patterns in this paper are similar to Turing patterns in the Gray-Scott (GS) reaction diffusion model [35] with parameter setting allowing for self-replicating patterns of spots. The GS model also allow for a metastable and spatially homogeneous state where local perturbation can trigger production of new spots that spreads out and eventually fills the entire space. A difference from this paper is that the GS system does not have long range interaction. The dots are generated in the fashion of cell division due to the local reaction, which renders the self-replicated spots lacking intrinsic size uniformity and long-range order. In

contrast, the long-range interaction in this paper prescribes an intrinsic size scale that ensures highly uniform and ordered patterns.

IV. CONCLUSION

In summary, we proposed a mechanism that self-assembly can propagate spontaneously and deliver ordering information to distance. This mechanism utilizes the ordered pattern in the growth front to trigger self-assembly in the affected zone. Two propagation modes: diffusion-limited and activation-limited, were identified. We showed that the propagation can produce extremely long-range ordered superlattice. While a representative system with dipole-type interaction was considered, we envision that the mechanism may be applicable to a wide range of self-assembly systems.

ACKNOWLEDGMENTS

The authors acknowledge financial support from National Science Foundation Award No. CMMI-0700048.

References

- [1] G. M. Whitesides, and B. Grzybowski, *Science* **295**, 2418 (2002).
- [2] R. Klajn, K. J. M. Bishop, M. Fialkowski, M. Paszewski, C. J. Campbell, T. P. Gray, and B. A. Grzybowski, *Science* **316**, 261 (2007).
- [3] J.-M. Nam, C. S. Thaxton, and C. A. Mirkin, *Science* **301**, 1884 (2003).
- [4] J. Liu, and Y. D. Li, *Advanced Materials* **19**, 1118 (2007).
- [5] E. V. Shevchenko, D. V. Talapin, N. A. Kotov, S. O'Brien, and C. B. Murray, *Nature* **439**, 55 (2006).
- [6] D. Nykypanchuk, M. M. Maye, D. van der Lelie, and O. Gang, *Nature* **451**, 549 (2008).
- [7] H. Chik, J. Liang, S. G. Cloutier, N. Kouklin, and J. M. Xu, *Appl. Phys. Lett.* **84**, 3376 (2004).
- [8] S. Pierrat, I. Zins, A. Breivogel, and C. Sonnichsen, *Nano Lett.* **7**, 259 (2007).
- [9] M. J. Fasolka, and A. M. Mayes, *Annu. Rev. Mater. Res.* **31**, 323 (2001).
- [10] T. L. Morkved, M. Lu, A. M. Urbas, E. E. Ehrichs, H. M. Jaeger, P. Mansky, and T. P. Russell, *Science* **273**, 931 (1996).
- [11] R. Plass, N. C. Bartelt, and G. L. Kellogg, *J. Phys.: Condens. Matter*, 4227 (2002).
- [12] R. Plass, J. A. Last, N. C. Bartelt, and G. L. Kellogg, *Nature* **412**, 875 (2001).
- [13] J. C. Love, L. A. Estroff, J. K. Kriebel, R. G. Nuzzo, and G. M. Whitesides, *Chemical Reviews* **105**, 1103 (2005).
- [14] W. Lu, and D. Salac, *Phys Rev Lett* **94**, 146103 (2005).
- [15] J. Y. Cheng, C. A. Ross, H. I. Smith, and E. L. Thomas, *Advanced Materials* **18**, 2505 (2006).
- [16] J. Xu, S. Park, S. L. Wang, T. P. Russell, B. M. Ocko, and A. Checco, *Adv. Mater.* **22**, 2268 (2010).
- [17] A. Ghadimi, L. Cademartiri, U. Kamp, and G. A. Ozin, *Nano Lett.* **7**, 3864 (2007).
- [18] M. E. Leunissen, H. R. Vutukuri, and A. v. Blaaderen, *Adv. Mater.* **21**, 3116 (2009).
- [19] J. S. Langer, *Science* **243**, 1150 (1989).
- [20] A. L. Garner, Y. Y. Lau, D. W. Jordan, M. D. Uhler, and R. M. Gilgenbach, *Cell Proliferation* **39**, 15 (2006).
- [21] M. G. Vicker, *Exp. Cell Res.* **275**, 54 (2002).
- [22] W. Hordijk, and M. Steel, *J. Theor. Biol.* **227**, 451 (2004).
- [23] J. Billingham, *Nonlinearity* **17**, 313 (2004).
- [24] M. C. Cross, and P. C. Hohenberg, *Rev. Mod. Phys.* **65**, 851 (1993).
- [25] J. F. Douglas, K. Efimenko, D. A. Fischer, F. R. Phelan, and J. Genzer, *Proc. Natl. Acad. Sci.* **104**, 10324 (2007).
- [26] J. Claret, J. Ignés-Mullol, R. Reigada, F. Sagues, and J. Crusats, *Phys. Rev. E* **73**, 026225 (2006).
- [27] V. M. Kaganer, H. Möwald, and P. Dutta, *Rev. Mod. Phys.* **71**, 779 (1999).
- [28] A. B. Macisaac, K. De Bell, and J. P. Whitehead, *Phys. Rev. Lett.* **80**, 616 (1998).
- [29] W. Lu, and Z. Suo, *J. Mech. Phys. Solids* **49**, 1937 (2001).
- [30] K. Pohl, M. C. Bartelt, J. de la Figuera, N. C. Bartelt, J. Hrbek, and R. Q. Hwang, *Nature* **397**, 238 (1999).

- [31] C. P. Warren, G. Mikus, E. Somfai, and L. M. Sander, Phys. Rev. E **63**, 056103 (2001).
- [32] J. Riordan, C. R. Doering, and D. ben-Avraham, Phys. Rev. Lett. **75**, 565 (1995).
- [33] H. Cook, Acta Metall **18**, 297 (1970).
- [34] K.-J. Lee, W. D. McCormick, J. E. Pearson, and H. L. Swinney, Nature **369**, 215 (1994).
- [35] Y. Nishiura, and D. Ueyama, Physica D: Nonlinear Phenomena **130**, 73 (1999).

Figure Captions

FIG. 1. Spontaneous propagation of self-assembly in a homogenous film. (a) The propagation was initiated by a local deposition at the left edge. The locally self-assembled structure as a precursor destabilized its initially stable surrounding areas through a dipole-type interaction. The newly formed structures inherited the same order information from the precursor and further activated the self-assembly of their neighbors. This process caused spatial extension of self-assembly and replication of the order, producing a long-range ordered superlattice without defects. (b) Magnified concentration field. (c) The corresponding I field is in phase with the pattern. $Q=1.8$, $\Omega=1.3$.

FIG. 2. (a) Free energy of homogenous film and dot pattern. The hexagonal dot pattern has lower energy when its average concentration is higher than a critical value, C_D . The range between C_D and C_L is a bistable state, where a homogenous film is stable against small perturbation although the dot pattern has lower energy. (b) Illustration of free energy change during perturbation growth. The ordered pattern in the growth front removes the energy barrier, Δg_b , in the affected zone, causing a homogenous film (H) to self-assemble into a dot pattern (D). $Q=1.8$, $\Omega=1.3$.

FIG. 3. Growth of dot superlattice by propagation of self-assembly (superlattice length normalized by the diameter of a dot). The upper curve shows activation-limited propagation. $Q=1.8$, $\Omega=1.3$. The lower curve shows long range diffusion-limited propagation. $Q=1.7$, $\Omega=1.4$. The inset illustrates propagation accompanied by long-range diffusion. The average

concentration of the dot pattern, C_p , is higher than C_0 , while the average concentration in the affected zone, C_a , is less than C_0 . The concentration gradient drives long-range diffusion from the remote area in the homogenous film to the affected zone by a diffusion distance d .

FIG. 4. Propagation of self-assembly in two-dimensions. $Q=1.8$, $\Omega=1.3$.

Figures

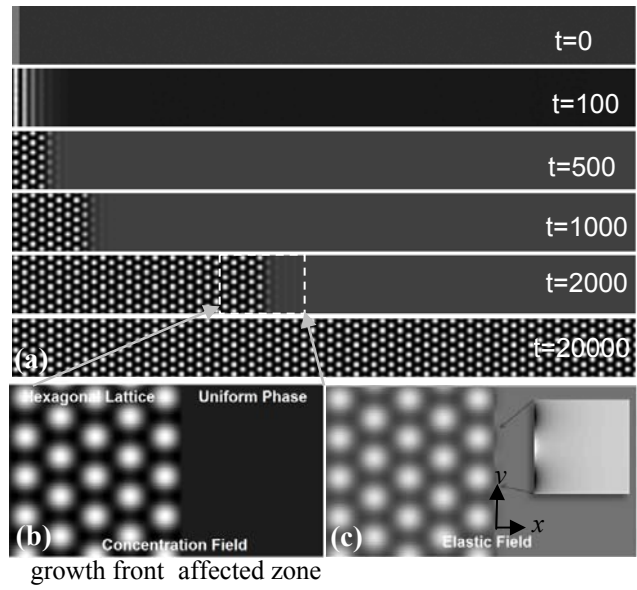


FIG. 1

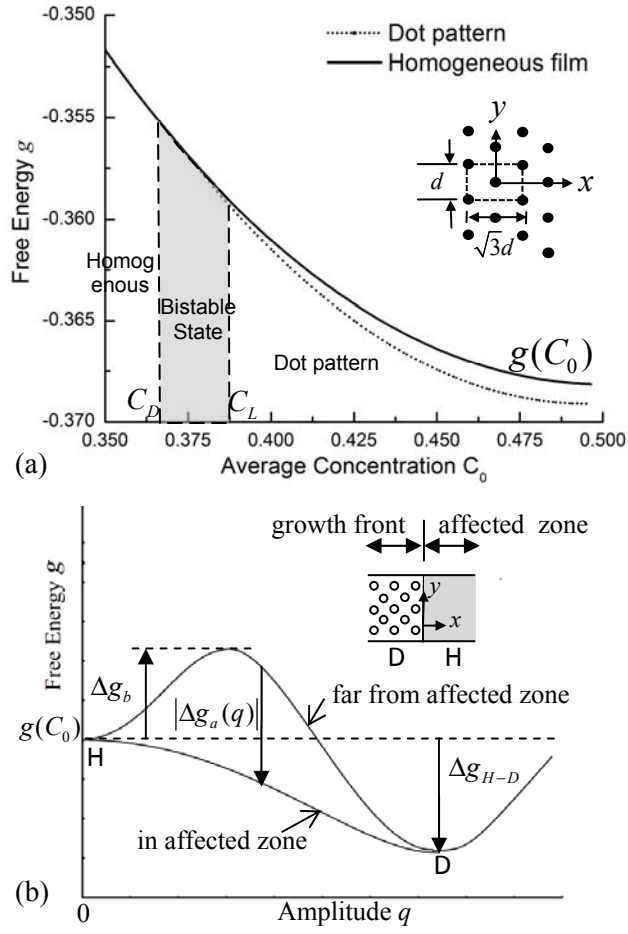


FIG. 2

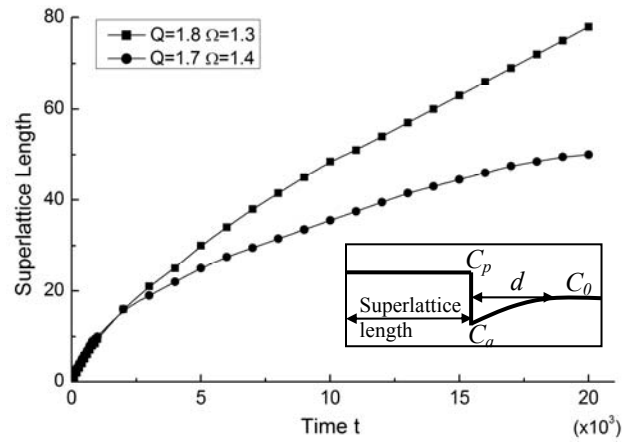


FIG. 3

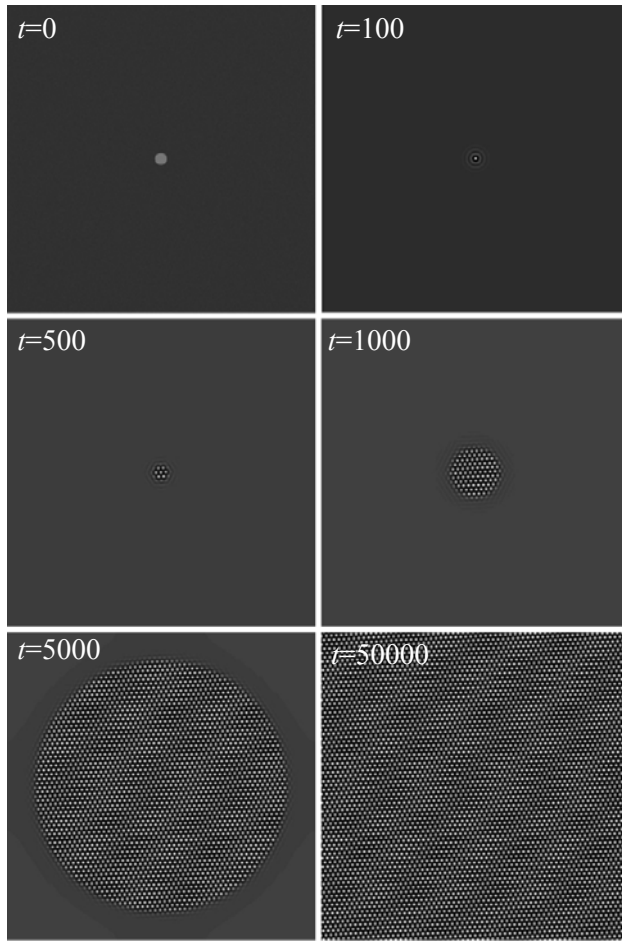


FIG. 4